Correction strategy for infants' diffusion-weighted images corrupted with motion

J. Dubois[1,2], G. Dehaene-Lambertz[1,3], L. Hertz-Pannier[2,4], G. Santoro[1], J-F. Mangin[3,5], and C. Poupon[3,5]
[1]U562, Inserm, Gif-sur-Yvette, France, [2]LBIOM, CEA, Gif-sur-Yvette, France, [3]IFR49, Paris, France, [4]U663, Inserm, Paris, France, [5]LNAO, CEA, Gif-sur-Yvette, France

Introduction

In the developing brain, non-invasive Diffusion Tensor Imaging (DTI) and High Angular Resolution Diffusion Imaging (HARDI) provide crucial information on the early organization of white matter bundles [1,2] and monitor the progressive maturation and myelination of functional networks [3,4]. However these techniques are difficult to implement in non-sedated babies because of motion sensitivity. Here we propose a post-processing methodology for correcting diffusion-weighted (DW) images from motion artifacts, before the computation of diffusion maps.

Materials and Methods

Problematic In DTI and HARDI, DW images are currently acquired along several orientations of the diffusion gradients taken on a single shell in the Q-space. Increasing the orientation count provides a more precise spatial estimation of the diffusion model and a higher signal-to-noise ratio (SNR) of the resulting diffusion maps, better than averaging. But it also increases the acquisition time, implying that motion is more likely. Therefore a compromise between image quality and acquisition time may be found. In EPI, motion has two consequences: artifacts in the slices acquired during any motion and misregistration of the volumes localization afterwards. A simple way to get rid of the first artefacts is to throw away the corresponding corrupted volumes. Our alternative strategy is to take advantage of the high diffusion orientation count to correct for corrupted images.

Principle of the motion outliers correction The basic concept is to compare, for each slice independently, the DW image for the orientation O_i to the b=0 image and to all the other 29 orientations (O_j, $j \neq i$), in order to detect for motion-artifacted slices and to correct them. To do so, the coefficient of Mutual Information (MI) between the DW O_i image and the b=0 image is computed (as it does not impose any linear relationship between the two images, thus making the measurement independent of the gray level intensity that is variable across orientations). The mean and standard-deviation (StdDev) of MI coefficients over all orientations are calculated. For outlier detection, the O_i image is considered as an outlier if its MI coefficient is not in the range: Mean $\pm$ f x StdDev, where the factor f can be adjusted. For a given slice location, several DW images for different Oi may be corrupted. As the acquisitions are performed on a single shell, the signal at each voxel can be decomposed on a modified spherical harmonics (SH) basis, as described in [5]. In our case, we process the decomposition from the set of non-corrupted DW images. Then, the previous SH coefficients can be used to infer the signal values along the orientations corresponding to outliers, thus replacing the corrupted DW images.

MR acquisition The study was performed on 15 infants born at term (mean age: 13±4.2weeks, range: 5.9w-21.4w), under a protocol approved by the Institutional Ethical Committee. Infants were spontaneously asleep during MR imaging, and particular precautions were taken to minimize noise exposure, by using customized headphones and covering the magnet tunnel with some special noise protection foam. Acquisitions were realized on a 3T MRI system (Siemens Tim Trio, Erlangen), equipped with a whole body gradient (40mT/m, 200T/m/s) and a 32-channel head coil. A DW spin-echo single-shot EPI sequence, with parallel imaging (GRAPPA factor 2) and partial Fourier sampling (factor 6/8), was used to image 50 interleaved axial slices covering the whole brain with a 1.8mm isotropic spatial resolution (FOV = 23x23cm^2, matrix = 128x128, slice thickness=1.8mm). After the acquisition of the b=0 volume, diffusion gradients were applied along 30 orientations with b=700s.mm^{-2}, leading to a total acquisition time of 5min40s (TE=72ms, TR=10s).

Motion correction strategy We implemented a 3-step correction strategy based on BrainVISA/PTK tools [6]. First, we corrected the most corrupted slices (black strips) with the above outlier methodology applied with f=3. Second, we corrected the 3D motion and the eddy-current distortions: we registered each DW volume (50 slices) to the b=0 volume using a MI criteria with an affine transformation. We also applied the corresponding rotation to the assigned diffusion orientation. Third, we corrected the remaining corrupted slices (minor strips) with the outlier methodology using a lower factor f=2.

DTI post-processing and tractography Afterwards, the diffusion tensor parameters were estimated in each voxel using PTK and BrainVISA software [6]. Maps of mean (<D>), longitudinal ($\lambda_{//}$) and transverse ($\lambda_{\perp}$) diffusivities, fractional anisotropy (FA) and color-encoded directionality (RGB) were generated. 3D tractography was performed using regularized particle trajectories [7], from a whole-brain mask excluding voxels with low FA (<0.15) or high <D> (>2.10^{-3}mm^2.s^{-1}). We further focused on the corpus callosum, since its reconstruction is hardly reliable in infants because of partial volume effects with the ventricles [3]. Fiber selection regions were selected in the inter-hemispheric plane, and splitting regions were positioned 5mm away in both hemispheres [3]. Quantification of diffusion indices was performed on average over the resulting tracts of the genu, splenium and body [3].

Results

High-quality DW images were acquired in all infants (mean SNR measured on b=0 image in frontal white matter: 171±38). Because of small movements during their sleep, we observed reduced motion artifacts in 8/15 infants, concerning no more than 7/30 orientations. The application of our motion correction strategy enabled the correction of all corrupted slices (Figure 1a-b), and the reliability of DTI maps was increased (Figure 1c-d). For the babies who did not move at all, it implied no changes in DTI maps. Using successive steps, with decreasing f factor and 3D registration, enabled to homogenize the MI coefficients over the 30 orientations (Figure 2). For all infants, the corpus callosum was reliably reconstructed (Figure 3a). Age-related changes were observed in its body and splenium (for <D>, $\lambda_{\perp}$ and FA), but not in its genu (Figure 3b).

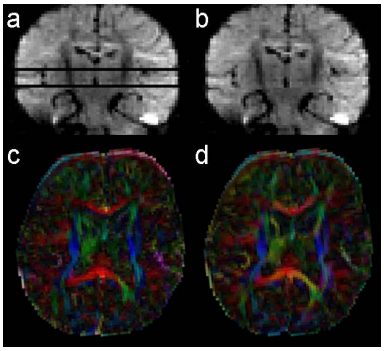

Figure 1: DW images without correction (a) and after correction of outlier slices (b). RGB maps obtained after exclusion of 5 outlier volumes (c) or correction of outlier slices (d).

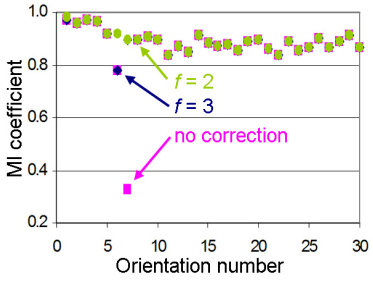

Figure 2: MI coefficient between DW and b=0 images along the 30 orientations, without correction or after outlier correction with f=3 2.

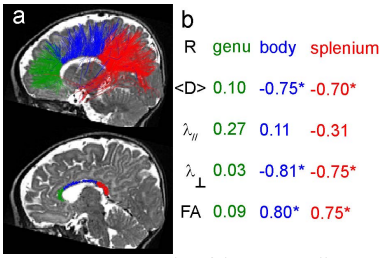

Figure 3: Tractography of the corpus callosum genu, body and splenium (a). Correlation coefficients of DTI indices and age (b: * significant at p<0.05).

Discussion and Conclusion

Our strategy was successfully used to correct DW sets of images corrupted by motion, which is frequent in non-sedated babies. The proposed method has the advantage of being fully automatic and reliable compared with the standard rejection of the whole volume even when a single slice is corrupted. Furthermore, it can be combined with DW acquisition strategies which optimize the spatial repartition of diffusion orientations with time and motion hypotheses [8]. In our infants group, we were able to reliably study the corpus callosum maturation with DTI indices. We did not observe age-related changes in the genu, probably because frontal fibers myelinate later on. In the body and splenium, $\lambda_{//}$ was not correlated with age as it fairly relies on fiber myelination [4].

References [1] Neil et al, NMR in Biomed 2002, 15:543-522. [2] Huppi et al, Pediatr Res 1998, 44:584-590. [3] Dubois et al, Hum Brain Map 2008, 29:14-27. [4] Dubois et al, J Neurosci 2008, 28:1943-1948. [5] Descoteaux et al, Med Image Anal 2009, 13:564-579. [6] Cointepas et al, Neuroimage 2003, 19:S810, http://brainvisa.info/. [7] Perrin et al, Inf Process Med Imaging 2005, 19:52-63. [8] Dubois et al, MAGMA 2006, 19:134-143.